https://scilett-fsg.uitm.edu.my/
Vol. 17(2) JUNE 2023

ISSN: 1675-7785
eISSN: 2682-8626

DOI:

Relaxivity Properties of Superparamagnetic Iron oxide Nanoparticles Incorporated into Silica Nanoparticles via Ultrasonic Irradiation

Bashiru Kayode Sodipo[1,2*], Willy Carreras Diaz[3], Abdul Aziz Azlan[2,4], Evelio Rafael Gonzalez Dalmau[5]

[1]Department of Physics, Kaduna State University, Nigeria

[2]School of Physics, Universiti Sains Malaysia, 11800 Pulau Pinang, Malaysia

[3]Biomedical Engineering, Polytechnic Institute José Antonio Echevarría, Cuba

[4]Nano-Biotechnology Research and Innovation (NanoBRI), Institute for Research in Molecular Medicine (INFORM), Universiti Sains Malaysia

[5]Departamento de Imágenes por Resonancia Magnética, Cuban Neurosciences Center, Street 190 e/25 and 27, Cubanacan Playa, Havana CP 11600, Cuba

Corresponding author: bashir.sodipo@kasu.edu.ng

Accepted: 12 May 2023; Published: 21 June 2023

ABSTRACT

Herein, we report the relaxivity property of Superparamagnetic Iron oxide Nanoparticles (SPION) incorporated into a silica nanoparticle framework. The SPION/Silica is synthesized via a non-seeded process of colliding as-synthesized SPION into a silica nanoparticle framework via ultrasonic irradiation. Both SPION and silica nanoparticles were synthesized independently. Then, the tremendous energy plus other unique conditions generated from ultrasonic irradiation were employed to accelerate, collide and incorporate SPION into silica nanoparticles. T_2 and T_1 relaxivity properties of the SPION/silica were measured in the Agarose gel phantom using a 1.5 T MRI scanner. Results revealed that the SPION/silica influence T_2 contrast in a concentration-dependent manner.

Keywords: *Nanoparticles; relaxivity, MRI contrast, SPION, silica, T1, T2, ultrasonic irradiation, sonochemical, incorporation.*

https://scilett-fsg.uitm.edu.my/
Vol. 17(2) JUNE 2023

ISSN: 1675-7785
eISSN: 2682-8626

DOI:

INTRODUCTION

Magnetic Resonance Imaging (MRI) dynamics are the excitation, resonance, and relaxation of hydrogen nuclei induced by the external magnetic field and radiofrequency (RF) pulse. Differences in Longitudinal (T_2) and Transverse (T_1) relaxation times are responsible for image contrast in MRI. T_2 and T_1 can be shortened by contrast agents (CA) to produce brighter and darker T_1 and T_2-weighted images. Superparamagnetic iron oxide nanoparticle (SPION) is typical nanoparticles with high relaxivity properties. However, owing to the need for surface modification of SPION with biocompatible substances, which can ensure colloidal stability and provide a binding site for bio-conjugation [1-3]. Several works have shown SPION/silica nanoparticles with good relaxivity properties [4-6]. Different wet chemical methods based on seed-mediated growth processes, such as sol-gel, microemulsions, and magnetic-mesoporous silica, have been used to synthesize SPION/silica as CA [7-9]. Due to surface effects and the high thickness of the silica shell, SPION/silica produced from these routes are less magnetic [10, 11] with poor relaxivity as MRI CA [12]. To minimize the surface effect of the silica coating on the magnetic and relaxivity properties, herein, we report the relaxivity property of SPION/silica synthesized via a non-seeded process of incorporating SPION into silica nanoparticles framework via ultrasonic irradiation. The sensitivity of the as-synthesized SPION/silica is determined in an Agarose gel phantom using a 1.5 T MRI scanner. Via this method of fabricating silica-coated SPION, our results demonstrate that a highly magnetic SPION/silica with excellent relaxivity can be produced.

EXPERIMENTAL

Ultrasonic Irradiation

Ultrasonic irradiation was carried out via a 13 mm diameter horn of 20 kHz Vibra-Cell ultrasonic. The Incorporation process involves three steps, as presented in the report [13], with slight modifications. First, SPION was synthesized by co-precipitating Fe^{3+} and Fe^{2+} at 2:1 with 1 M NaCl solution under a degassed environment, room temperature, and a pH of 10 [14]. The magnetic materials were washed and peptized in $HClO_4$. Second, silica nanoparticles were produced via the modified Stöber method by mixing 200 µL of 10 M ammonia with 200 mL distilled water and 6 mL of 1-butanol. Then, 2 mL of TEVS was added and agitated at 320 rpm and room temperature for one hour. Un-reacted chemicals were removed, and silica nanoparticles were purified through dialysis using a cellulose membrane for four days [15]. Finally, at a volume ratio 1:1, a mixture of SPION and silica nanoparticles' suspension was mixed, and pH was adjusted to 3.5 using NaOH solution. The mixture was ultrasonically irradiated for 30 minutes for heat dissipation in an iced bath environment. The nanoparticles were washed and separated using a magnet.

https://scilett-fsg.uitm.edu.my/
Vol. 17(2) JUNE 2023

ISSN: 1675-7785
eISSN: 2682-8626

DOI:

Relaxivity Property of SPION/Silica

Agarose gel phantom was prepared by dissolving 1 wt % Agarose XP in hot Milli-Q water [12]. The as-synthesized SPION/silica and 250 µL hot Agarose solutions were vortex-mixed in a glass vial and kept cool until they solidified. Four samples containing 1, 0.5, 0.25, 0.125, and 0 ml of SPION/silica were prepared and named Sample 1, Sample 2, Sample 3, Sample 4, and Sample 5, respectively. Sample 5 is a blank phantom and serves as a control of the experiment. Iron concentrations of samples 1-5 are determined using atomic absorption spectroscopy (AAS) as 1.587, 0.7935, 0.3968, and 0.1984 mM, respectively. MR images of the samples were obtained under a spin-echo sequence. For T_1, echo time (TE) is fixed at 10 ms, and repetition time (TR) is varied as 100, 150, 200, 300, 600, 1200, 2400, 4800, and 8000 ms. Similarly, for T_2, TR is fixed at 1000 ms, and TE is varied as 10, 15, 20, 30, 60, 120, and 200 ms. Other parameters, such as field of view (pov), image matrix, and slice thickness, are fixed at 340 mm, 256 x 128, and 3 mm, respectively.

Characterization

Morphology and elemental mapping were determined through electronic spectroscopy imaging (ESI) using energy filtering transmission electron microscopy (EFTEM) Zeiss Libra 120. Magnetization measurements were obtained via Vibrating Sample Magnetometer (VSM), and MR images were carried out with a 1.5 T MRI scanner (GE Healthcare).

RESULTS AND DISCUSSION

TEM micrographs of SPION and silica nanoparticles before ultrasonic irradiation are shown in Figures 1A and B, respectively. Silica nanoparticles and SPION sizes are ~50 and 10 nm, respectively. Ultrasonic irradiation of SPION in the presence of silica with tremendous power (~40 W), mechanical stirring, and other unique effects generated by the sonication induced random inelastic collision between SPION and silica nanoparticles. After the sonication period, SPION was found embedded in silica nanoparticles. The incorporation of SPION into silica nanoparticles can be related to the smaller size effect of SPION and mesoporous features of silica nanoparticles synthesized by the sol-gel method. Figure 1C is a micrograph of SPION/silica, which reveals that the silica shell is incorporated with multi-core SPION. We assumed that during ultrasonic irradiation of the samples, the SPION must have gained higher kinetic energy during the acceleration of the nanoparticles and coalesced into the silica via inelastic collision. Therefore, due to the smaller size of SPION, multiple SPION collided and penetrated the silica nanoparticles. Further characterization demonstrating the incorporation of SPION into silica nanoparticles is reported in [10].

The magnetization measurements of the samples are shown in Figure 2. The absence of hysteresis in the curves indicates that both naked SPION and SPION/silica nanoparticles were Superparamagnetic [16]. Saturated magnetization (M_s) of as-synthesized SPIONs and SPION/silica are 47.4 and 30 emu/g, respectively. The SPION/silica retains 63.29 % of its original Ms Values. From the high M_s of SPION/silica, we hypothesized that the ultrasound-assisted non-seeded process of incorporating SPION into the silica framework plays a vital role in preserving the magnetic moment of the core SPION.

https://scilett-fsg.uitm.edu.my/
Vol. 17(2) JUNE 2023

ISSN: 1675-7785
eISSN: 2682-8626

DOI:

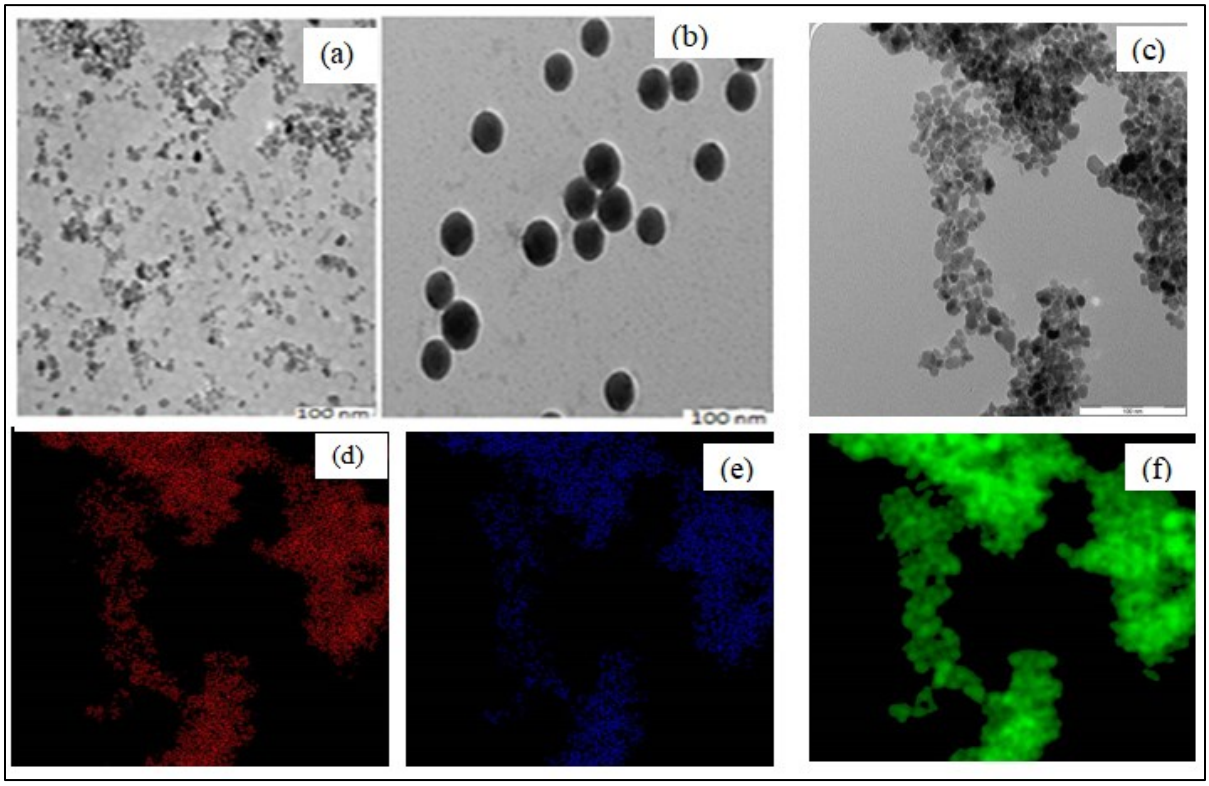

Figure 1: TEM micrograph of (a) SPION, (b) silica, (c) SPION/silica, (d) presence of silica coating is shown with the arrow

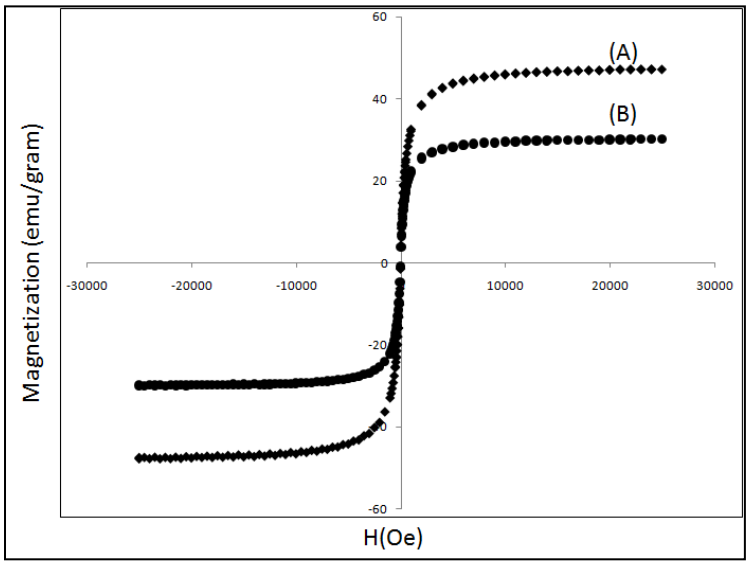

Figure 2: Showing room-temperature magnetization curve of (A) SPION and (B) SPION/silica nanoparticles

https://scilett-fsg.uitm.edu.my/
Vol. 17(2) JUNE 2023
ISSN: 1675-7785
eISSN: 2682-8626

DOI:

The relaxivity of SPION/silica is evaluated in gel phantom under spin-echo (SE) sequence. Agarose gel is well-known tissue equivalent MRI phantom. Like human tissue, it has a T_2 range of values (40–150 ms) [17]. However, its T_1 is inaccurate and incomparable to human tissue [18]. Via Equations 1 and 2, T_1 and T_2 can be determined by curve fitting [19]. Appropriateness and repeatability of these equations have been demonstrated in various studies [20 - 22].

$$S(t) = S_{\max}\left(1 - e^{-T_R/T_1}\right) \qquad \text{Equation 1}$$

$$S(t) = S_{\max} e^{-\frac{T_E}{T_2}} \qquad \text{Equation 2}$$

T_1 and T_2-weighted images of the samples are shown in Figure 3. Bright and dark images correspond to high and low relaxation times. T_2 of Samples 1-5 were evaluated as 1, 3.8, 4.1, 5.4, and 125.1 ms, respectively. Unlike effective shortening of T_2, T_1 of Sample 1-5 are 278.8, 516.3, 627.5, 755.9, and 6309.6 ms, respectively. The values are still very high. To determine the efficiency of SPION/silica as novel T_2 CA, relaxivities (r_2 and r_1) were determined using Equation 3.

$$1/T_{i,obs} = 1/T_{i,d} + r_i[M] \text{ (i = 1, 2)} \qquad \text{Equation 3}$$

Where $1/T_{i,obs}$, is the observed solvent relaxation rate in the presence of contrast agent, $1/T_{i,d}$ is the relaxation rate of pure diamagnetic solvent, and [M] is the concentration of the CA [21]. The sensitivity of T_2 CA can be determined from the ratio of r_2 to r_1; the higher the r_2/r_1, the better the CA efficacy [22]. The r_2, r_1, and r_2/r_1 of SPION/silica were evaluated as 288 $s^{-1}mM^{-1}$, 2 $s^{-1}mM^{-1}$, and 144, respectively. The r_2/r_1 result demonstrates the high sensitivity of SPION/silica.

https://scilett-fsg.uitm.edu.my/
Vol. 17(2) JUNE 2023

ISSN: 1675-7785
eISSN: 2682-8626

DOI:

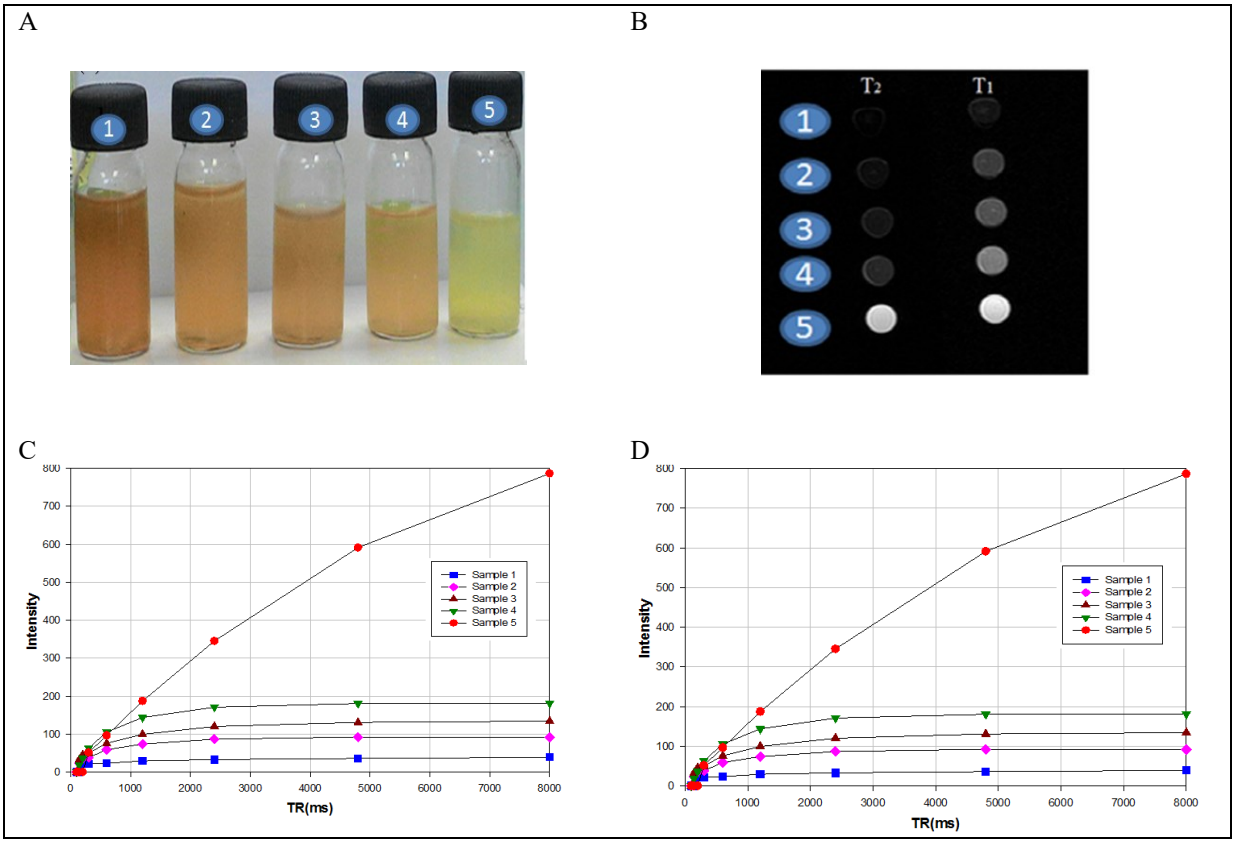

Figure 3: Showing (A) images of Sample 1-5 before MRI scan, (B) T1 and T2- weighted images of SPION/silica after scanning. Also, relaxometry fit curves of (C) T1 (D) T2

CONCLUSION

SPION is incorporated into silica nanoparticles via the ultrasound-assisted non-seeded method. This non-seeded method of coating silica on SPION allows the synthesis of highly magnetic SPION/silica nanoparticles. The SPION/silica nanoparticles showed high sensitivity and relaxivity as a novel MRI T_2 contrast agent.

ACKNOWLEDGMENTS

This work is supported by the Ministry of Education Malaysia (MoE) through Universiti Sains Malaysia FRGS grant 203/PFIZIK/6711351.

https://scilett-fsg.uitm.edu.my/
Vol. 17(2) JUNE 2023

ISSN: 1675-7785
eISSN: 2682-8626

DOI:

AUTHOR'S CONTRIBUTION

All authors equally contributed

CONFLICT OF INTEREST STATEMENT

The authors agree that this research was conducted without any self-benefits or commercial or financial conflicts and declare the absence of conflicting interests with the funders.

REFERENCES

[1] Noqta, O. A., Sodipo, B. K., & Aziz, A. A. (2020). One-pot synthesis of highly magnetic and stable citrate-coated superparamagnetic iron oxide nanoparticles by modified coprecipitation method. *Functional Composites and Structures*, *2*(4), 045005.

[2] Piché, D., Tavernaro, I., Fleddermann, J., Lozano, J. G., Varambhia, A., Maguire, M. L., ... & Grobert, N. (2019). Targeted T 1 Magnetic Resonance Imaging Contrast Enhancement with Extraordinarily Small CoFe2O4 Nanoparticles. *ACS applied materials & Interfaces*, *11*(7), 6724-6740.

[3] Braim, F. S., Ab Razak, N. N. A. N., Aziz, A. A., Ismael, L. Q., & Sodipo, B. K. (2022). Ultrasound-assisted chitosan-coated iron oxide nanoparticles: Influence of ultrasonic irradiation on the crystallinity, stability, toxicity, and magnetization of the functionalized nanoparticles. *Ultrasonics Sonochemistry*, *88*, 106072.

[4] Pinho, S. L., Laurent, S., Rocha, J., Roch, A., Delville, M. H., Mornet, S., ... & Geraldes, C. F. (2012). Relaxometric studies of γ-Fe2O3@ SiO2 core-shell nanoparticles: when the coating matters. *The Journal of Physical Chemistry C*, *116*(3), 2285-2291.

[5] Branca, M., Marciello, M., Ciuculescu-Pradines, D., Respaud, M., del Puerto Morales, M., Serra, R., ... & Amiens, C. (2015). Towards MRI T2 contrast agents of increased efficiency. *Journal of Magnetism and Magnetic Materials*, *377*, 348-353.

[6] Alzoubi, F. Y., Abu Noqta, O., Al Zoubi, T., Al-Khateeb, H. M., Alqadi, M. K., Abuelsamen, A., & Makhadmeh, G. N. (2023). A Novel One-Pot Synthesis of PVP-Coated Iron Oxide Nanoparticles as Biocompatible Contrast Agents for Enhanced T2-Weighted MRI. *Journal of Composites Science*, *7*(3), 131.

[7] Adam, A., & Mertz, D. (2023). Iron Oxide@ Mesoporous Silica Core-Shell Nanoparticles as Multimodal Platforms for Magnetic Resonance Imaging, Magnetic Hyperthermia, Near-Infrared Light Photothermia, and Drug Delivery. *Nanomaterials*, *13*(8), 1342.

[8] Pinho, S. L., Pereira, G. A., Voisin, P., Kassem, J., Bouchaud, V., Etienne, L., ... & Delville, M. H. (2010). Fine-tuning of the relaxometry of γ-Fe2O3@ SiO2 nanoparticles by tweaking the silica coating thickness. *ACS nano*, *4*(9), 5339-5349.

https://scilett-fsg.uitm.edu.my/
Vol. 17(2) JUNE 2023
ISSN: 1675-7785
eISSN: 2682-8626

DOI:

[9] Zhang, L., Wang, Y., Tang, Y., Jiao, Z., Xie, C., Zhang, H., ... & Zhang, C. (2013). High MRI performance fluorescent mesoporous silica-coated magnetic nanoparticles for tracking neural progenitor cells in an ischemic mouse model. *Nanoscale*, *5*(10), 4506-4516.

[10] Nemec, S., Kralj, S., Wilhelm, C., Abou-Hassan, A., Rols, M. P., & Kolosnjaj-Tabi, J. (2020). Comparison of iron oxide nanoparticles in photothermia and magnetic hyperthermia: Effects of clustering and silica encapsulation on nanoparticles' heating yield. *Applied Sciences*, *10*(20), 7322.

[11] Yuan, Y., Rende, D., Altan, C. L., Bucak, S., Ozisik, R., & Borca-Tasciuc, D. A. (2012). Effect of surface modification on magnetization of iron oxide nanoparticle colloids. *Langmuir*, *28*(36), 13051-13059.

[12] Lassenberger, A., Scheberl, A., Stadlbauer, A., Stiglbauer, A., Helbich, T., & Reimhult, E. (2017). Individually stabilized, superparamagnetic nanoparticles with controlled shell and size leading to exceptional stealth properties and high relaxivities. *ACS applied materials & interfaces*, *9*(4), 3343-3353.

[13] Sodipo, B. K., & Aziz, A. A. (2015). Non-seeded synthesis and characterization of superparamagnetic iron oxide nanoparticles incorporated into silica nanoparticles via ultrasound. *Ultrasonics sonochemistry*, *23*, 354-359.

[14] Sodipo, B. K., & Aziz, A. A. (2014). A sonochemical approach to the direct surface functionalization of superparamagnetic iron oxide nanoparticles with (3-aminopropyl) triethoxysilane. *Beilstein Journal of Nanotechnology*, *5*(1), 1472-1476.

[15] Sodipo, B. K., & Aziz, A. A. (2020). Optimization of sonochemical method of functionalizing Amino-Silane on superparamagnetic iron oxide nanoparticles using Central Composite Design. *Ultrasonics sonochemistry*, *64*, 104856.

[16] Sodipo, B. K., Noqta, O. A., Aziz, A. A., Katsikini, M., Pinakidou, F., & Paloura, E. C. (2023). Influence of capping agents on fraction of Fe atoms occupying octahedral site and magnetic property of magnetite (Fe3O4) nanoparticles by one-pot co-precipitation method. *Journal of Alloys and Compounds*, *938*, 168558.

[17] Kharey, P., Goel, M., Husain, Z., Gupta, R., Sharma, D., Manikandan, M., ... & Gupta, S. (2023). Green synthesis of biocompatible superparamagnetic iron oxide-gold composite nanoparticles for magnetic resonance imaging, hyperthermia and photothermal therapeutic applications. *Materials Chemistry and Physics*, *293*, 126859.

[18] Mitchell, M. D., Kundel, H. L., Axel, L., & Joseph, P. M. (1986). Agarose as a tissue equivalent phantom material for NMR imaging. *Magnetic resonance imaging*, *4*(3), 263-266.

[19] Hellerbach, A., Schuster, V., Jansen, A., & Sommer, J. (2013). MRI phantoms–are there alternatives to agar?. *PloS one*, *8*(8), e70343.

[20] Qodarul, M. R., Silvia, L., Zainuri, M., & Dwihapsari, Y. (2023, May). The effect of repetition time variation on quantitative T1 magnetic resonance imaging on Agar. In *AIP Conference Proceedings* (Vol. 2604, No. 1). AIP Publishing.

[21] Hernandez, D., & Kim, K. N. (2023). Use of machine learning to improve the estimation of conductivity and permittivity based on longitudinal relaxation time T1 in magnetic resonance at 7 T. *Scientific Reports*, *13*(1), 7837.

[22] Qin, J., Laurent, S., Jo, Y. S., Roch, A., Mikhaylova, M., Bhujwalla, Z. M., ... & Muhammed, M. (2007). A high-performance magnetic resonance imaging T2 contrast agent. *Advanced Materials*, *19*(14), 1874-1878.